Available online at www.sciencedirect.com

ScienceDirect

IFAC PapersOnline CONFERENCE PAPER ARCHIVE

IFAC PapersOnLine 58-25 (2024) 67–72

Modelling of consumer dynamics to improve fuel gas blending control

M.D. Sibiya * **A.J. Wiid** * **J.D. le Roux** * **I. K. Craig** *,1

* *Department of Electrical, Electronic, and Computer Engineering, University of Pretoria, Pretoria, South Africa.*

Abstract: Although fuel gas systems represent a large part of industrial chemical processes, there has been limited literature on their modelling and control. The available literature typically neglects the effects of fuel gas consumer dynamics, leaving much of the system's important dynamic behaviour omitted. This paper aims to contribute to the existing literature on fuel gas control and improve an existing fuel gas control benchmark problem by including the effects of fuel gas consumer dynamics on the system. Two model predictive controllers (MPC) were designed, where the first MPC uses a model that neglects the consumer dynamics and the second MPC uses a model that includes the consumer dynamics. It was found that the MPC neglecting consumer dynamics has a pressure variability 5.8 times higher than the MPC that includes the dynamics. It also has a relative sensitivity index (RSI) of 7.2, indicating the presence of model-plant mismatches (MPM) affecting controller performance.

Keywords: Consumer dynamics; Fuel gas blending; Furnace control; High heating value; Model predictive control; Model-plant mismatch.

1. INTRODUCTION

A large part of chemical industries such as oil, gas and petrochemicals use fuel gas as their primary energy source. In refineries, the largest energy consumers are fired heater units with approximately 65 – 90% of the refinery's heating provided by furnaces that use fuel gas (Masoumi and Izakmehri, 2011). Other fuel gas consumers include steam boilers and fired heater reboilers used on the various refinery distillation columns (Brooks et al., 2014). Due to the large consumption of fuel gas, minor optimisation improvements can lead to significant economic and environmental benefits as well as improved factory wide stability.

The fuel gas system typically receives two types of feed streams:

- a blend of purchased make-up/enrichment streams such as natural gas (NG), and
- "off-gases" from other units within the chemical complex that would have otherwise been flared.

Typically, the off-gases have a lower calorific value (High Heating Value (HHV)) and high variability in composition and availability. Therefore, the make-up streams must always be added to the blend to maintain the correct quality and quantity supply of fuel gas (Brooks et al., 2014; Muller et al., 2011; Ricker et al., 2012). The optimisation objective is to use as much off-gases as possible while maintaining the quality specifications. This results in the reduction of expensive make-up gas purchases and reductions in total gases burnt across the factory.

Although representing a large part of an industrial chemical process, there is limited literature on the control of fuel gas systems. The literature available typically neglects the effects of consumer dynamics (Muller et al., 2011; Ricker et al., 2012). This leaves a large portion of the system's dynamic behaviour omitted. The literature typically models the effects on the header pressure from all feed streams as the same. This is not a reflection of reality, as each stream has a different effect on the HHV of the fuel gas. A decrease in the HHV will result in consumers demanding more fuel gas to maintain the same heating duty. This causes a secondary effect where the pressure of the fuel gas header starts decreasing. The reverse case is also valid for streams that increase the HHV. These secondary effects significantly affect the overall pressure control of the unit.

Muller et al. (2011) focused on modelling and validating an industrial fuel gas blending system and applying advanced control on the system. The controller model gains were iteratively updated from a developed first-principle nonlinear model. The work by Muller et al. (2011) was further expanded by Ricker et al. (2012) to include continuous variations on the feed gas compositions and 23 discrete disturbances, such as reductions in the availability of off-gas streams and changes in the load demand.

Brooks et al. (2014) use the patented methods and software described by Dreyer and Kotze (2007) to optimise the fuel gas blending system of a 90 000-bpd refinery in Cape Town, South Africa, as part of an overall Energy and Emissions Optimisation (EEO) project. Brooks et al. (2014) include the effects of consumer dynamics on the fuel gas pressure. This was achieved by using "shadow variables" to model the secondary effects of flow changes from each feed stream on the blended HHV. This, in turn, impacts the pressure demand from consumers. The pressure is effectively modelled as the sum of the real

[1] Corresponding author. E-mail: ian.craig@up.ac.za

10.1016/j.ifacol.2024.10.239

manipulated variables (MVs) response and the shadow MVs response.

The contribution of this paper is the improvement of an existing fuel gas control benchmark problem (Ricker et al., 2012) by including the effects of fuel gas consumer dynamics on the system. The effects of model-plant mismatch due to missing consumer dynamics on the controller models of a model predictive controller (MPC) are also highlighted.

2. CURRENT MODEL

The fuel gas model in this study is based on the model developed by Muller et al. (2011). This model was developed using step test data from an industrial fuel gas system for the dynamics, and a nonlinear first-principle model linearised at the nominal operating range. The same model is used as a benchmark problem by Ricker et al. (2012). The fuel gas system aims to keep the header pressure (y_P) within limits while maintaining the fuel gas specifications. These specifications are fuel gas HHV (y_{HHV}), Wobbe Index (y_{WI}), and Flame Speed Index (y_{FSI}). This is achieved by blending the six feed streams (F_i), namely, NG (F_1), Reformed Gas (RG) (F_2), Hydrogen (H_2) (F_3), Nitrogen (N_2) (F_4), Tail Gas 1 (TG_1) (F_5), and Tail Gas 2 (TG_2) (F_6). Table 1 shows the validated model linearised at nominal plant conditions. The time units have been converted from hours, as in the original work, to minutes to better suit the rest of the models in this work.

As can be seen from the last row in Table 1, the effects from the various F_i to y_P all have the same model. In general, however, each F_i will either increase or decrease y_{HHV}. This causes a secondary effect where y_P starts to change due to the difference in fuel gas flow rate demand ($F_{FG_{Demand}}$) from consumers based on y_{HHV} changes.

3. CONSUMER MODEL

The consumer model developed here is based on furnace behaviour as furnaces and fired heaters represent 65 – 90% of a refinery's fuel gas usage (Masoumi and Izakmehri, 2011). These furnaces are typically under closed-loop proportional-integral(-derivative) (PI(D)) control with the outlet temperature controller writing to the fuel gas pressure/flow controller/valve. A decrease in y_{HHV} causes the furnace outlet temperature (T_{OUT}) to decrease. This results in the feedback temperature controller demanding more fuel gas to maintain T_{OUT} at setpoint. Note that the y_{HHV} to consumer $F_{FG_{Demand}}$ dynamic model is based on the behaviour of the feedback controller.

Figure 1 shows the block diagram of furnace control and fuel gas interactions. The block diagram includes a Smith Predictor as a result of the long deadtimes present in furnace outlet temperature control loops (Feliu-Batlle and Rivas-Perez, 2020, 2021; Rivas-Perez et al., 2014). For Figure 1, $T_{SP}(t)$ is the setpoint of $T_{OUT}(t)$, $e(t)$ is the furnace temperature controller error, $u(t)$ is the controller output to manipulate the fuel gas valve and $d(t)$ is the y_{HHV} disturbance on $T_{OUT}(t)$. The various Laplace models are described below.

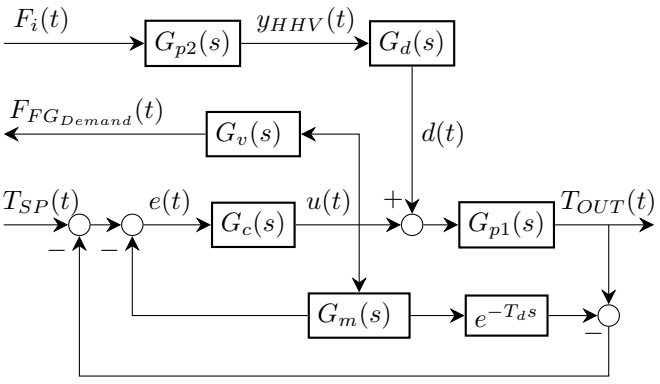

Fig. 1. Furnace temperature control to HHV disturbances

3.1 $G_{p1}(s)$: Fuel gas valve to furnace outlet temperature model

The fuel gas valve to T_{OUT} model is based on Rivas-Perez et al. (2014) and Feliu-Batlle and Rivas-Perez (2021) which was obtained from step test data on an industrial crude oil preheating furnace.

$$G_{p1}(s) = \frac{T_{OUT}(s)}{U(s) + D(s)} = \frac{3.66e^{-1.83s}}{(1 + 0.853s)(1 + 0.202s)} \quad (1)$$

Other literature that contains a similar model form for fuel gas burning applications includes Feliu-Batlle and Rivas-Perez (2020), who modelled an industrial cement rotary kiln.

3.2 $G_{p2}(s)$: Fuel gas feed stream(s) to fuel gas HHV model

Models of the six F_i streams to y_{HHV} are given in the first row of Table 1. The gains and directions change based on the current y_{HHV} and F_i compositions (Muller et al., 2011; Ricker et al., 2012). Iterative gain updates are necessary as process conditions change.

3.3 $G_d(s)$: HHV disturbance model

To calculate the disturbance gain at the nominal region used for the model identification of Table 1, the fuel gas demand duty (Q_{Demand}) is calculated as

$$Q_{Demand} = y_{HHV} F_{FG_{Demand}} \quad (2)$$

Taking the derivative of (2) with respect to time gives:

$$\frac{dQ_{Demand}}{dt} = \frac{dy_{HHV}}{dt} F_{FG_{Demand}} + \frac{dF_{FG_{Demand}}}{dt} y_{HHV} \quad (3)$$

Assuming a constant duty demand $\frac{dQ_{Demand}}{dt} = 0$, the change in $F_{FG_{Demand}}$ with respect to changes in y_{HHV} is calculated as

$$\frac{dF_{FG_{Demand}}}{dy_{HHV}} = -\frac{F_{FG_{Demand}}}{y_{HHV}} \quad (4)$$

Table 1. Original fuel gas model linearised at nominal operating conditions

	NG (F_1)	**RG** (F_2)	**H₂** (F_3)	**N₂** (F_4)	**TG₁** (F_5)	**TG₂** (F_6)
y_{HHV}	$\frac{0.86}{2.10s+1}e^{-0.33s}$	$\frac{-0.19}{2.60s+1}e^{-0.33s}$	$\frac{-0.19}{2.27s+1}e^{-0.33s}$	$\frac{-0.57}{2.60s+1}e^{-0.33s}$	$\frac{-0.13}{2.33s+1}e^{-0.33s}$	$\frac{-0.07}{2.65s+1}e^{-0.33s}$
y_{WI}	$\frac{1.07}{2.09s+1}e^{-1.00s}$	$\frac{-0.27}{2.57s+1}e^{-1.00s}$	$\frac{0.09}{2.28s+1}e^{-1.00s}$	$\frac{-1.32}{2.61s+1}e^{-1.00s}$	$\frac{-0.16}{2.34s+1}e^{-1.00s}$	$\frac{-0.11}{2.63s+1}e^{-1.00s}$
y_{FSI}	$\frac{-2.07}{2.10s+1}e^{-0.33s}$	$\frac{0.48}{2.62s+1}e^{-0.33s}$	$\frac{1.19}{2.21s+1}e^{-0.33s}$	$\frac{-1.46}{2.61s+1}e^{-0.33s}$	$\frac{0.39}{2.25s+1}e^{-0.33s}$	$\frac{0.10}{2.71s+1}e^{-0.33s}$
y_P	$\frac{18.67}{s}$	$\frac{18.67}{s}$	$\frac{18.67}{s}$	$\frac{18.67}{s}$	$\frac{18.67}{s}$	$\frac{18.67}{s}$

Using the nominal values of $F_{FG_{Demand}} = 30$ and $y_{HHV} = 17.25$ (Muller et al., 2011) the gain is calculated as 1.739. $G_d(s)$ is then modelled using the calculated gain and the furnace HHV disturbance dynamics from Rivas-Perez et al. (2014) and Feliu-Batlle and Rivas-Perez (2021) as

$$G_d(s) = \frac{D(s)}{y_{HHV}} = \frac{-1.739}{(1+0.167s)} \tag{5}$$

3.4 $G_v(s)$: Fuel gas valve opening to flow demand model

The model for the fuel gas valve opening to $F_{FG_{Demand}}$ is

$$G_v(s) = \frac{F_{FG_{Demand}}(s)}{U(s)} = \frac{1}{0.167s\ +\ 1} \tag{6}$$

3.5 $G_c(s)$: Controller model

$F_{FG_{Demand}}$ dynamics will ultimately depend on the behaviour of the controller. Two furnace control schemes are modelled. The first scheme is a standard PI controller, and the second scheme a PI controller with a Smith predictor, as shown in Figure 1. The predictor model $G_m = \frac{T_{OUT}(s)}{U(s)}$ is the delay-free part of (1), and the deadtime T_d is equal to the delay in (1). Table 2 shows the tuning parameters used for the model simulation.

Table 2. Tuning parameters

	PI	**PI$_{\text{Smith}}$**
K_C	0.1	0.48
$\tau_I(min)$	1.33	1

Figure 2 and 3 show how the two controllers behave and affect $F_{FG_{Demand}}$. The first part is a response to a setpoint change from 280 $°C$ to the nominal furnace operating temperature of 390 $°C$ at $t = 0$ s. After 1000 s, the NG stream is stepped up by 10 kNm^3/h, which changes y_{HHV} and causes a disturbance to the furnace leading to a load change in $F_{FG_{Demand}}$ to maintain the duty required to keep T_{OUT} at setpoint.

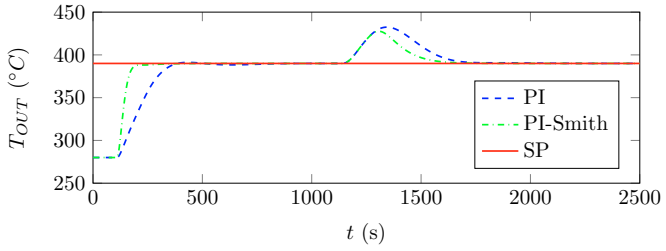

Fig. 2. Furnace outlet temperature control using a PI controller vs. a PI-Smith predictor controller.

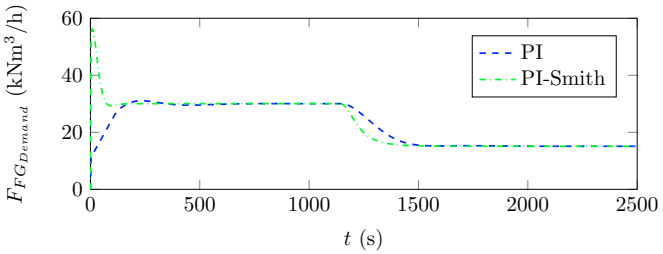

Fig. 3. Fuel gas demand using a PI controller vs. a PI-Smith predictor controller.

3.6 Fuel stream(s) to fuel gas demand model due to HHV changes

The F_i to $F_{FG_{Demand}}$ models are derived from the transfer function block diagram shown in Figure 1 using system identification. Table 3 shows the models obtained when the PI-Smith predictor controller described in Section 3.5 is used. These models are used in the MPC simulation studies described in Section 4.

3.7 Fuel stream(s) to fuel gas pressure model

The final F_i to y_P models combine the pressure changes due to F_i flow rate changes, and changes in y_{HHV} which affects $F_{FG_{Demand}}$. The combined model equations are shown in Table 4.

Figure 4 shows three step responses for each F_i to y_P. The dotted blue line (G_1) represents y_P changes due to F_i flow rate changes only. This is the default model (last row of Table 1) and is the same for all inlet streams. The dotted green line (G_2) represents y_P changes due to the changing $F_{FG_{Demand}}$ caused by changes in y_{HHV} after F_i is changed. This is obtained by multiplying G_1 with the models in Table 3 and changing the sign since the demand is the outlet of the fuel gas. The solid red line (G) represents the final y_P model, which is a combination of G_1 and G_2 as indicated in Table 4.

Figure 4 shows that the consumer dynamics play a significant role in the actual effects a change in each F_i will have on y_P. The most significant effects are noticed in the models from NG and N_2. For the NG model the actual pressure (G) is almost twice as large as the initial model pressure (G_1) after 1000 s. At steady state the actual gain, which is the slope, is 2.5 larger than the original gain of the model. The actual N_2 model exhibits first-order behaviour, and does not act as an integrator like G_1. This is because N_2 has no heating value, and at steady state, increasing the N_2 feed stream will continue to cause the same demand from the other streams as before. $F_{FG_{Demand}}$

Table 3. Fuel streams to fuel gas demand models

	NG (F_1)	**RG** (F_2)	**H₂** (F_3)	**N₂** (F_4)	**TG₁** (F_5)	**TG₂** (F_6)
FG_{Demand}	$\frac{-1.5e^{-2.25s}}{0.905s^2+2.54s+1}$	$\frac{0.332e^{-2.25s}}{1.11s^2+3.04s+1}$	$\frac{0.332e^{-2.25s}}{0.97s^2+2.71s+1}$	$\frac{1e^{-2.25s}}{1.12s^2+3.05s+1}$	$\frac{0.223e^{-2.25s}}{0.992s^2+2.77s+1}$	$\frac{0.127e^{-2.25s}}{1.15s^2+3.09s+1}$

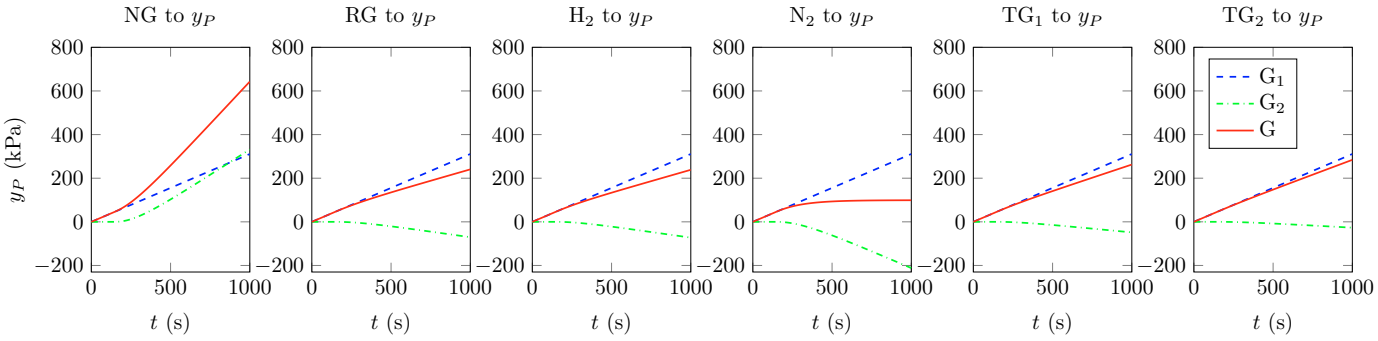

Fig. 4. Combined pressure effects.

Table 4. Final combined pressure model

Stream	y_P
NG (F_1)	$\frac{18.67}{s}(1+\frac{1.5}{0.905s^2+2.54s+1}e^{-2.25s})$
RG (F_2)	$\frac{18.67}{s}(1-\frac{0.332}{1.11s^2+3.04s+1}e^{-2.25s})$
H₂ (F_3)	$\frac{18.67}{s}(1-\frac{0.332}{0.968s^2+2.71s+1}e^{-2.25s})$
N₂ (F_4)	$\frac{18.67}{s}(1-\frac{1}{1.12s^2+3.05s+1}e^{-2.25s})$
TG₁ (F_5)	$\frac{18.67}{s}(1-\frac{0.223}{0.992s^2+2.77s+1}e^{-2.25s})$
TG₂ (F_6)	$\frac{18.67}{s}(1-\frac{0.127}{1.15s^2+3.09s+1}e^{-2.25s})$

will just increase by the same amount as N_2 increases, and hence the first-order behaviour.

The combined pressure models shown in Table 4 are simplified using system identification in order to ease the implementation of the MPC controller described in Section 4. Table 5 shows the final updated y_P models used in the MPC design.

4. MPC CONTROLLER DESIGN

To compare how consumer dynamics affect the performance of the fuel gas system's control, three cases using MPC are compared. The first case (MPC_{1_Design}) uses the models given in Table 1 as both the controller and plant models. This represents the design case if consumer dynamics are neglected. The second case (MPC_{1_MPM}) uses the models from Table 1 as controller models, and the y_P models from Table 5 as the plant models. This case includes model-plant mismatch (MPM), and represents the case where the controller of Muller et al. (2011) and Ricker et al. (2012) is implemented when consumer demand varies.

The final case (MPC_2) uses the models from Table 5 for both the controller and plant models. This is the design case if consumer dynamics are included.

4.1 MPC tuning

All cases were given the same tuning parameters to ensure that only the effect of including/excluding consumer dynamics is studied. The controllers are implemented using the MATLAB MPC toolbox (Bemporad et al., 2024), and hence, the tuning parameters are based on the MATLAB MPC implementation.

MPC tuning parameters are given in Table 6. The controller sampling time was chosen as 0.25 min. The control horizon was chosen as 10 intervals, and the prediction horizon was chosen as 60 intervals (15 min) to cover the longest model settling time. The controlled variables (CVs) and MVs minimum and maximum limits were kept the same as Muller et al. (2011), and the scaling factors were chosen as the spans of the limits. For MVs, all scale factors were taken as the highest span (30). Scaling is used since the MATLAB MPC internal equations employ dimensionless signals (Bemporad et al., 2024).

The CV limits are set as soft constraints obtained by applying an Equal Concern Relaxation (ECR) value of 0.01. This prevents the QP solution from being infeasible when not all hard constraints can be mathematically achieved. The weights of the CVs are set giving the highest priority to maintaining y_{HHV} closer to the nominal value than the other CVs. The pressure has the least priority and is allowed to float more than the other CVs.

All MV rate weights are set as 1 to penalise large MV moves. No limit is set for the MV maximum moves. The weight is the penalty for the deviation of MVs/CVs from their target/reference. Typically, NG, RG, and N_2 are purchased streams which a fuel gas controller tries to minimise. Muller et al. (2011) and Ricker et al. (2012) achieved this by setting the targets of these MVs to 0 and setting the weight equal to the costs of each stream. However, the focus of this study is on quantifying the effects of MPM, therefore no weights were added on the MVs to allow the controller to always be able to keep all CVs at or close to their target.

5. MPC SIMULATION RESULTS

Figures 5 and 6 show the performance for the three cases. The system is initially started at the nominal values MVs = $[2.17, 0, 1.23, 0, 0, 26.6]^T$, CVs = $[17.25, 26, 42.5, 2100]^T$ and setpoint (target) changes are made to all CVs in a sequential manner. The step sizes are 10% of the CVs

Table 5. Updated fuel gas pressure models including consumer dynamics

	NG (F_1)	**RG** (F_2)	**H_2** (F_3)	**N_2** (F_4)	**TG_1** (F_5)	**TG_2** (F_6)
y_P	$\frac{46.8}{s(2.92s+1)}$	$\frac{12.7(4.52s+1)}{s(1.1s+1)^2}$	$\frac{12.7(4.35s+1)}{s(1.09s+1)(s+1)}$	$\frac{106}{(3.03s+1)(0.21s+1)}$	$\frac{14.7(3.09s+1)}{s(0.96s+1)(0.85s+1)}$	$\frac{16.5(2.14s+1)}{s(0.77s+1)(0.73s+1)}$

Table 6. MPC variable tuning parameters

	Min	**Max**	**Scale Factor**	**Weight**	**Rate Weight**
Inputs (MVs)					
NG	0	15	30	0	1
RG	0	20	30	0	1
H_2	0	5	30	0	1
N_2	0	5	30	0	1
TG_1	0	30	30	0	1
TG_2	0	30	30	0	1
Outputs (CVs)					
y_{HHV}	16.5	18	1.5	10	-
y_{WI}	25	27	2	8	-
y_{FSI}	39	46	7	7	-
y_P	2 000	2 200	200	2	-

range. After the system has stabilised from the last target change, an unmeasured disturbance is introduced into the system by increasing the amount of Q_{Demand} by 10%. The controllers must then return the CVs back to their desired targets.

The simulation results show that for identical tuning settings, MPC_{1_Design} and MPC_2 have similar behaviour/performance regardless whether the system has consumer dynamics or not. This is due to both systems having no MPM and also identical models for the other CVs. However, once consumer dynamics are introduced as would be the case on an actual plant, the controller performance will deteriorate. MPC_{1_MPM} has an underdamped response due to the consumer dynamics causing MPM. The oscillating behaviour of the controller can increase/decrease depending on how aggressively tuned the controller is. Tuning the controller more robustly would result in less oscillations and decreased controller performance when compared to MPC_2.

6. QUANTIFYING THE IMPACT OF MPM ON PERFORMANCE

The results obtained from the simulations are quantified using the method proposed by Badwe et al. (2010). For the analysis, the system variable and models were first scaled based on the ranges given in Table 6 to all have a range of -1 to 1. A brief explanation of the method is given below and Table 7 gives the performance indicators for the three cases that were simulated.

Badwe et al. (2010) uses a relative sensitivity index (RSI), designed sensitivity index (DSI) and variability ratio (VR) to identify MPM and quantify the effects it has on controller performance. This is based on using closed-loop process data with sufficient setpoint/target changes in the data and comparing the achieved process behaviour against the design behaviour which does not have MPM.

RSI is the ratio of the achieved controller error reduction over the designed controller error reduction. A value of RSI $\neq 1$ indicates the presence of MPM influencing controller performance. If RSI > 1, it means that the MPM is causing poor performance since the current achieved control error is greater than the designed control error.

DSI is a measure of how well the controller is tuned and a smaller value indicates that the controller is robust. Typically, for a scaled system, a DSI value greater than 2 indicates an aggressively tuned controller. Presence of MPM can affect the DSI and cause it to increase. If RSI > 1 and DSI is also large, the effects of MPM can be amplified by an aggressive controller. VI is a ratio of the achieved variability of the CVs over the designed variability. VI > 1 indicates that the CV has an increased variability as compared to the controller design.

Table 7. Quantification of MPM for fuel gas system

		y_{HHV}	y_{WI}	y_{FSI}	y_P
MPC_{1_Design}	RSI	1.00	1.00	1.00	1.00
	DSI	1.62	1.96	1.56	1.72
	VI	1.02	1.01	1.03	1.01
MPC_{1_MPM}	RSI	1.00	1.00	1.00	7.19
	DSI	1.61	2.00	1.56	1.83
	VI	1.04	1.03	1.11	5.83
MPC_2	RSI	1.00	1.00	1.00	1.00
	DSI	1.62	1.95	1.56	1.63
	VI	1.03	1.02	1.04	1.02

Results from Table 7 confirm the observation made earlier that MPC_{1_Design} and MPC_2 have similar performance due to the absence of model mismatches. For MPC_{1_MPM} the RSI for y_P is 7.2, indicating the presence of MPM on the CV and indicating that the achieved error reduction is larger than the ideal designed system which does not consider the consumer dynamics. The DSI for y_P in MPC_{1_MPM} is also larger than the design case, which indicates that the controller is more aggressive on the actual system with MPM than the design case. VI is 5.8 times larger indicating increased variability. These results indicate that the MPC_{1_MPM} controller needs to be detuned in order to provide improved control under MPM.

7. CONCLUSION

Consumer dynamics on fuel gas systems significantly affect the controller and plant's behaviour. In this study, the most significant effect was noticed in the NG and N_2 to y_P models, where the actual model gain is 2.5 times as large as the original NG model and the N_2 model changes from an integrating to a self-regulatory model. For identical tuning, the MPC that neglects consumer dynamics on the controller models has an underdamped/oscillating response compared to the controller that includes the consumer dynamics. The VI of this controller is 5.8 times larger than the controller that includes the dynamics. RSI is also 7.2 times larger resulting in an increase in DSI. Depending on the severity, the oscillating behaviour could result in reduced stability of the fuel gas system that will negatively impact downstream consumers.

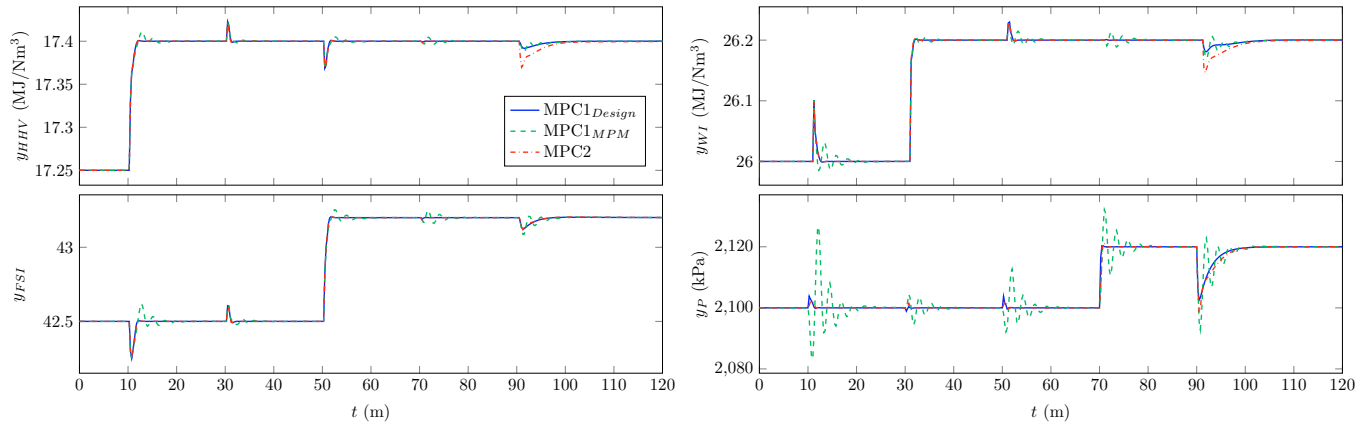

Fig. 5. Plant outputs for the three simulated MPC cases.

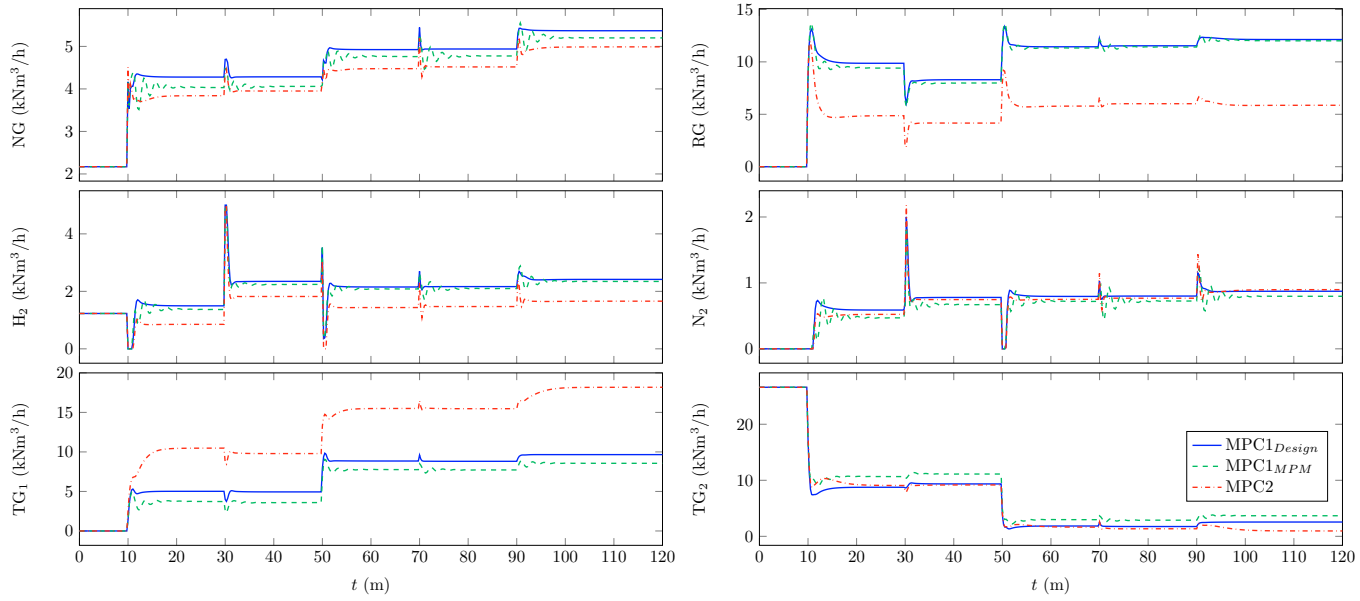

Fig. 6. Controller moves for the three simulated MPC cases.

Future work includes expanding the control design to the non-linear model case, incorporating the HHV as an internal MPC variable for improved pressure prediction and investigating scenarios where one or more MVs are constrained as in the benchmark problem (Ricker et al., 2012).

REFERENCES

Badwe, A.S., Patwardhan, R.S., Shah, S.L., Patwardhan, S.C., and Gudi, R.D. (2010). Quantifying the impact of model-plant mismatch on controller performance. *Journal of Process Control*, 20(4), 408–425.

Bemporad, A., Ricker, N., and Morari, M. (2024). *Model Predictive Control Toolbox^{TM} User's Guide*. The MathWorks, Inc.

Brooks, K., Carr, A., Dreyer, R., and Maksa, M. (2014). Energy and emissions optimisation at Chevron Cape Town. *IFAC Proceedings Volumes*, 47(3), 1278–1283.

Dreyer, R.P. and Kotze, G.D. (2007). Methods, systems, and articles for controlling a fluid blending system. US Patent 7,188,637.

Feliu-Batlle, V. and Rivas-Perez, R. (2020). Design of a robust fractional order controller for burning zone temperature control in an industrial cement rotary kiln. *IFAC-PapersOnLine*, 53(2), 3657–3662.

Feliu-Batlle, V. and Rivas-Perez, R. (2021). Control of the temperature in a petroleum refinery heating furnace based on a robust modified Smith predictor. *ISA Transactions*, 112, 251–270.

Masoumi, M. and Izakmehri, Z. (2011). Improving of refinery furnaces efficiency using mathematical modeling. *International Journal of Modeling and Optimization*, 1, 74–79.

Muller, C., Craig, I., and Ricker, N. (2011). Modelling, validation, and control of an industrial fuel gas blending system. *Journal of Process Control*, 21(6), 852–860.

Ricker, N., Muller, C., and Craig, I. (2012). Fuel gas blending benchmark for economic performance evaluation of advanced control and state estimation. *Journal of Process Control*, 22(6), 968–974.

Rivas-Perez, R., Feliu-Batlle, V., Castillo-Garcia, F., and Benitez-Gonzalez, I. (2014). Temperature control of a crude oil preheating furnace using a modified Smith predictor improved with a disturbance rejection term. *IFAC Proceedings Volumes*, 47(3), 5760–5765.